Mar 7th, 8:00 AM

Environmental Parameters of an Aborted Launch

Cyril N. Golub
Pan American World Airways, Inc.

ENVIRONMENTAL PARAMETERS OF AN ABORTED LAUNCH

Cyril N. Golub
Pan American World Airways, Inc.
Patrick Air Force Base, Florida

Summary

Constituents of the pressure environment of an aborted launch include the unbalance of the atmospheric pressure caused by the blast and the pressure differentials developing across structures due to the rapid succession of overpressures and underpressures of the shockfront as it spreads through the launch complex.

The main features of the thermal environment are the fireball, its heat output, and the values, distribution, and duration of the ambient temperatures.

The knowledge of the behavior of the pressure and thermal environments of an aborted launch is a starting point for the engineering design or evaluation of materials, assemblies, or systems which might be exposed to the abort environment and are expected to survive.

This paper describes the first known measurement and interpretation of abort data. The occasion was the accidental disintegration of the Atlas-Centaur vehicle at the Cape Kennedy Air Force Station, Florida, on 2 March 1965. Other applications of launch hazards instrumentation are discussed.

Introduction

Several coordinated study and experimental programs are expanding our knowledge of launch hazards, their mechanisms and effects. Interest in this field is shared and sponsored by the U. S. Air Force, the U. S. Atomic Energy Commission and the National Aeronautics and Space Administration. Results from these programs are used by these and other agencies which are involved in national aerospace undertakings. The overall basic objective of the launch hazards assessment program is the development of a reliable method (mathematical model) for predicting the damage potential that a missile or space vehicle accident at launch can create in its vicinity. The stepping stones leading to the fulfillment of this objective are several theoretical and experimental investigations, the main ones being Project PYRO, concerned with the blast hazards of liquid propellants, and Project SOPHY, concerned with the failure mechanisms of solid propellants. Results from both theoretical studies and controlled explosion experiments have to be verified and extended by data obtained from actual full-scale accidents.

A significant contribution to the acquisition of full-scale data points was made by a first-time measurement of a full set of the environmental parameters of a launch abort. The approach used in the design of the data acquisition instrumentation and in the interpretation of the acquired data is based on the measurement and analysis of "environmental effects"; the mechanism of the basic phenomena can then be inferred from these measured effects.

In this paper, we shall first examine the observed effects of the Atlas-Centaur abort on 2 March 1965. We shall then turn our attention to the actual measurements, how they were obtained, and how they were interpreted. We shall conclude with remarks on launch hazards instrumentation that we have available for these and other measurements.

For the purpose of this paper, we have tried to select the most illustrative material and to concentrate on the insight that users can gain into the environmental mechanisms involved; greater emphasis has been placed on what the abort environment looks like as revealed by the measurements made than on what the instruments registered; a complete set of numerical values can be found in the references.

The Measured Environment

A number of different presentations can be made of the data acquired during the Atlas-Centaur abort; the attempted launch was designated Test 205. Only the more significant data presentations are discussed in this paper.

Pressure Effects

The measurement and analysis of the shockwaves, their propagation pattern, their intensities and velocities have led to this overall effect in the area of complex 36A (Figure 1). The inset in Figure 1 will help us define the main shockwave parameters that we shall be using in this presentation. They are labeled as follows:

1. Shockfront: ideally a steep straight front of the advancing shockwave.

2. Arrival time: time at which the shockfront reaches a given point.

3. Peak overpressure: maximum positive unbalance of the ambient atmospheric pressure created by the passage of the shockwave.

4. Positive phase and positive phase or overpressure duration: the time that the atmospheric unbalance remains positive or above the

normal atmospheric pressure which existed before shockwave arrival.

5. Negative phase or underpressure: the partial lowering of the atmospheric pressure to below that existing before shockwave arrival.

6. Impulse: the area under the positive phase curve or time integral of the overpressure pulse.

The lines of equal pressure or isobars in Figure 1 represent the maximum peak overpressure levels reached along these isobars as the shockwave due to the third and most powerful explosion was traveling across the complex. This particular event was selected as an example because it was the only high-order explosion during the abort and the only one to give rise to a well defined shockwave. This set of isobars depicts one set of environmental pressure effects due to the aborted launch:

1. The maximum overpressures reached at any point of the complex showing the progressive decay of the intensity of the shockwave as it spread across the complex.

2. The distribution of these values around the complex; this distribution is peculiar to the particular failure mode involved and is not likely to occur in the same pattern in some other accident; however, the assumed reasons for the shape of the distribution and the passive indicators confirming the measured values give valuable insight into the phenomenon for future application in the launch hazards assessment program.

3. The corresponding underpressures have been tabulated rather than plotted.

4. The time duration of the over and under pressures have also been tabulated rather than plotted.

5. The impulse together with overpressure has been plotted on Figure 2 as a function of range and pressure gauge location.

When first initiated, the deflagration started spreading in the northwesterly direction and was fairly well contained in the other sectors. This initial asymetrical heating of the atmosphere apparently provided a preferential propagation path for the shockwave giving the shockfront the assumed profile shown in Figure 3 at a given instant of time and resulting in the pattern shown in Figure 1. The passive indicators of shockwave intensity consists of floodlights, windows, masonry walls, honeycomb structures distributed throughout the complex, which did or did not break, crack or collapse (Figures 4 and 5) depending on whether or not the shockwave intensity was high enough to cause the damage. Figure 1 shows that this damage pattern essentially confirms the isobar pattern derived from the overpressure measurements. Having defined what we see in Figure 1, we can step back and examine the overall picture. Upon the initiation of an explosion or of each explosion, since there may be a multiplicity of explosions, a shockwave starts traveling across the complex as a growing bulbous shape more or less distorted by the features of the "terrain" which the atmospheric medium is. The shockfront of the bubble will spread faster for instance in the direction in which there is preheating of the air; it will spread slower elsewhere and when contained by physical obstacles such as the remaining skin of the vehicle or the umbilical tower. It took a little less than one second for the shockwave to clear the complex. The time would have been shorter had the shock been more intense.

There is a sudden rise in pressure at the shock front immediately followed by a rarefaction. The "peak-to-peak" change in pressure from positive to negative and its short duration is basically the damage mechanism which affects structures. Its intensity decays as the shockfront spreads away from the source. The damage listed in Figure 1 would have been found at greater distances had the explosion been more intense and the damage at close range would have been more extensive. Damaging effects can also extend further if focusing is present as was apparently the case in this example. The blast overpressure was of the order of 200 psi at the vehicle interface and had decreased to 2 psi along an ellipse with a 500 ft. minor axis and a major axis of over 1000 ft. A 2 psi overpressure is sufficient to break a concrete block wall.

The way the chemical energy contained in a space vehicle propellant system can be dissipated as a result of an accident will be discussed after we examine the thermal environment.

Thermal Effects

Our main interest lies in determining the heat output of the burning fuel and in getting some idea of the dynamics of the fireball - fireball motion, temperature gradients, time history of the fire. This kind of knowledge, just as the knowledge of the behavior of the pressure environment, is a starting point for the engineering design or evaluation of materials, assemblies, or systems which might be exposed to the abort environment and are expected to survive.

At its inception, the fire broke out just above the launch deck and spread down into the flame bucket and formed a fireball above the deck. The heat reached its peak at the top of the umbilical tower two to three seconds later than on the launch deck. Then it decayed after an equal length of time; as the fireball expanded and moved across the complex, the only fire left near the launch point was due to the

RP-1 fuel spilled on the launch deck and lasted for over an hour generating a moderate amount of heat. Figure 6 shows typical temperature time histories.

The fireball passed by and singed the service tower and then gradually dissipated after having reached an ellipsoidal shape 800 feet long, 300 feet wide, and 450 feet high. The peak temperature reached 6000°F, while the peak rate of heat output was approximately 425 BTU/ft^2-sec.

Pressure and Thermal Energy of the Propellant

The chemical energy stored in the fuel is dissipated as pressure energy and thermal energy. The ratio between the two depends on a number of factors such as physical containment, mixing ratios and rates, and other conditions collectively described as failure modes.

Our description of the pressure and thermal effects can be summed up by saying that in this particular abort there was relatively little pressure energy generated while most of the propellant energy was dissipated thermally. The low pressure yield of this abort was further confirmed by the absence of ground motion detected by the local US Coast and Geodetic Survey seismic stations.

Environmental Measurements

The raw data which led to the interpretation results presented in the preceding sections were acquired with an instrumentation system called the Pad Abort Measuring System or PAMS.

Instrumentation System

As stated previously, the measurement philosophy of PAMS is based on defining the environmental parameters of an aborted launch by working back from the pressure and thermal data recorded during an abort. The system data acquisition capabilities are listed in Figure 7.

The pad-abort measuring system consists of contact-type sensors and a recording ground station. The sensors are located so that they will be in contact with or in the immediate vicinity of the abort environment if the abort occurs on or near the launch pad. The connection between sensors and the ground station is by hard-wire. The ground station is located in the corresponding blockhouse.

Pressure Sensors - The pressure phenomena are monitored by an array of pressure sensors. The layout of the array is based on a spacing scheme designed to provide independent readings and on considerations of expected lack of symmetry in the pressure distribution, both in range and in azimuth. The result is a spiral centered about the launch pad, with sensors located at the intersection of the spiral and two perpendicular axes drawn through the launch pad (Figure 8). The perspective view on the figure shows pressure gauges 4 through 11 in the field while gauges 1, 2, 3 and the high-sensitivity gauge 12 are located on the launch deck.

The high-pressure sensors are close to the expected location of the source, and the most sensitive sensor is near the perimeter of the complex. There are 11 sensors with a maximum range varying between 20,000 and 1 psi and an additional 1-psi sensor on the launch stand to measure normal launch overpressures. The pressure sensors are bridge-type variable reluctance transducers, driven by a 3-kc carrier. The output is an AM signal, with a zero amplitude when the bridge is balanced and an amplitude proportional to pressure when the arm of the bridge coupled to the sensing diaphragm is unbalanced by an overpressure.

Thermal Sensors - Temperatures are sensed by the four thermocouples of different characteristics. Thermal energy (the total heat output) is sensed by a radiometer and a calorimeter. There are two assemblies, each made up of four thermocouples, a radiometer, and a calorimeter. One assembly is at the base of the umbilical tower; the other one is mounted on the umbilical to extend data acquisition time as the fireball rises (Figure 9). Depending on the exact location of the source and on the particular point in time, the thermal assemblies may or may not be enveloped in the fireball. To ensure survival of the instrumentation and cabling, the base of the sensors and the cable are water cooled. The four thermocouples have different characteristics (see inset in Figure 6). The most sensitive of the thermocouples, a tungsten-tungsten-rhenium thermocouple in a thin tantalum case, can follow the steep rise of the expected thermal pulse (its time constant is 10 milliseconds) but may disintegrate short of its maximum temperature range of 5400 °F because of its fragility. A tungsten-tungsten-rhenium thermocouple encased in siliconized molybdenum for greater protection has a slower response but will survive longer and will typically follow the peak and some of the decay of the pulse. Slow-response but high-survivability platinum-platinum-rhodium and chromel-alumel thermocouples housed in a stainless steel case measure the end of the decay and the steady state temperature. Their temperature ranges are 3300°F and 2650°F, respectively.

A Naval Radiological Laboratory radiometer senses thermal radiant energy up to 800 BTU/ft^2-sec, while a calorimeter picks up both radiant and convective energy of the order of 500 BTU/ft^2-sec. The partially redundant characteristics of the sensors are a result of their different degrees of survivability and their overlapping ranges for continuous coverage. The signals from the sensors are low-level DC; they are amplified by DC amplifiers

located immediately below the launch stand before being fed to the ground station tape recorder.

Calibration - Predetermined simulated pressure and temperature signals can be remotely applied to the system at the location of each sensor so that the whole system can be calibrated at once from sensor to recording tape.

Running Time - Because the initiation and the nature of the phenomena is unpredictable, the requirement of recording the event from its very significant beginning has been solved by starting recording before the inception of any hazardous sequence and continuing recording for up to three hours. After three hours, a quick change of tape reels gives an additional three hours. The process can be repeated as many times as required. Thus the lengthiest operations, including any likely holds, can be monitored.

Photography - Documentary and engineering sequential photographic coverage supplies the size and rate of growth of the fireball and occasional evidence of the dynamic forces involved.

Raw Data

The types of data measured and recorded by PAMS are listed in the following table:

Pressure Data	Thermal Data
Arrival Times	Temperatures vs. time (°F)
Pressure Pulse Rise Time (msec)	Heat flux ys. time (BTU/ft²-sec)
Peak Overpressure (psi)	
Overpressure vs. time (psi)	
Negative pressure phase vs. time (psi)	

Only a review of the acquired data will be given here since this topic is covered in detail in References 1 and 2.

Pressure Data - A composite tracing of the pressure history at each of the active pressure gauges is shown in Figure 10.

The labeling of this figure makes most of its information self-explanatory. Insert A shows the pressure variations recorded by Pressure Gauge 12 during booster pulsation and shutdown approximately two seconds before the first major explosion (explosion 3 on the figure).

Inset B shows a break in PG #12 trace; this can be reasonably interpreted as another explosion in spite of the excessive stress damage to this gauge during "explosion 3". The amplitude value is probably unreliable. A total of six weak and strong shockwaves, either incident or reflected, were recorded.

The values of pressure, arrival times, and other information are tabulated and commented upon in References 1 and 2.

Thermal Data - A composite tracing of some of the temperatures registered at the two stations (top of umbilical and launch deck) is shown in Figure 11. A complete discussion of the thermal data can also be found in Reference 2.

More will be said about the pressure and thermal data in the next section on interpretation.

Data Analysis and Interpretation

Data reduction routines include reading numerical values from oscillographic transcriptions of the magnetically recorded data, and deriving the different quantities of interest. Again in this paper the more routine aspects of the subject are mentioned only briefly since they are covered in detail in the quoted references. More emphasis is put upon the insight that can be gained from the analysis and interpretation of the reduced data. The first section on the "Measured Environment" went to some length in the qualitative description of the abort environment. Some of the deductive processes leading to such a description and confirming the high level of confidence in the results will now be examined.

Pressure

We are more concerned with the characteristics of shock propogation rather than those of the detonation process. The quantity of the charge is the governing parameter in this case. The total weight of the RP-1/LOX combination in this case was approximately 8.5 times that of the LH_2/LOX propellant. Furthermore, LH_2/LOX can be shown by theoretical analysis to have only a slightly greater explosive potential. It can be concluded that the principal shock was produced by the RP-1/LOX propellant.

Let us introduce Figure 12 here. It shows the plot of relative shockfront velocity vs. horizontal range. The relative shockfront velocity as it is used here is the excess of shockfront velocity over the local sound velocity, a concept somewhat similar to air speed as applied to an aircraft. The shockfront velocity values were computed by inserting the pressures values recorded by PAMS into the usual Hugoniot equations. The corresponding relative velocities were then calculated and plotted as a function of range in Figure 12. The point corresponding to pressure gauge #3 can be brought onto the curve if the assumption is made that this gauge measured a face-on rather than a side-on overpressure and if the appropriately corrected value is used in the calculations. Reference 1 explains why this assumption is valid. The relative shape and slope of the curve are in complete agreement with results from a controlled LOX/RP-1

test (Reference 3). The extrapolation to a range of 5 feet of the curve joining the measured points brings it to a point representing the value of the relative shock velocity at the vehicle interface derived analytically from the detonation properties of the RP-1/LOX propellant. The point above it gives the corresponding value for a LH_2/LOX combination. Here again is an indication that the RP-1/LOX propellant had a major role in this explosion. The consistency of the results having been established this far, we now proceed to plot overpressures values vs. range from the shock characteristics derived in Figure 12. This plot is shown in Figure 13. Figure 12 also shows the variation of overpressure vs. range for a TNT surface burst. The comparison between this curve and that for the detonation characteristics of RP-1/LOX illustrates the doubtful value of the TNT equivalency concept without careful qualifications of the conditions under which a certain equivalency is established.

Considerations similar to those described in this section can be applied to other parameters of interest and have the virtue of allowing not only to reconstruct the basic mechanisms involved but also to validate consistent data and eliminate spurious measurements.

Thermal

In a similar manner, thermal quantities of interest can be derived and validity of the measurements established. To illustrate the techniques used here, consider again Figure 11.

Assuming that the data from the fastest response thermocouple (channel 5) represented the effective radiating temperature of the ambient gas, their values were used as the input to thermal models of the other three thermocouples; they each have different thermal response characteristics and are all located at the top of the umbilical tower (channels 6, 7, 8). An analog computer was used to determine the theoretical responses of these three thermocouples. Figure 11 illustrates the agreement between measured and calculated data. The figure indicates that the umbilical tower temperatures peaked at over 6000°F and then rapidly decreased to near normal as the fireball dissipated.

Let us examine now the temperatures recorded by the channel 9 thermocouple which is located on the launch deck and has characteristics identical to those of the channel 6 thermocouple so that their readings are directly comparable. It can be seen that for the first five seconds or so their responses are very similar with the difference that the peak temperature was reached on the launch deck approximately three seconds before the same occurred on the umbilical tower. However, after the initial similarity, the temperature on the launch deck remained between 1500°F and 2000°F indicative of the residual fire from the fuel spilled on the deck, while the temperature at the umbilical station dropped back to normal within a very short time.

Using similar heat transfer programs and again assuming that temperature channel 5 represents the effective radiating temperature within the fireball, it is possible to estimate the peak heat output from the fireball. A value of 425 BTU/ft^2-sec is thus obtained and can then be compared to radiometer and calorimeter readings.

Characteristics of PAMS sensors are sufficiently different either by their physical location or by their response that reasonably independant readings are obtained; different analytical approaches can then be used to compare and validate these readings. By the same token, there is enough redundancy that failure of several channels does not prevent a meaningful representation of an abort environment from being obtained.

Other Launch Hazards Instrumentation

The preceeding sections described the application of the Pad Abort Measuring System to the acquisition of the environmental parameters of an aborted launch. This system is mobile and services any of fourteen complexes at the Cape Kennedy Air Force Station. It has also been used to measure the environmental parameters of a normal launch, especially in the pressure area: for instance, damaging pressures and their time history at various critical locations on a complex during the launch of a large booster.

A remote reading pyrometer is also in operation to measure rocket exhaust temperatures with an accuracy of better than 50°C; it is used with a sampling rate of the order of 100 samples per second which can be increased or decreased.

Another launch hazard related to the launch of large boosters is the intense acoustic field generated by the propellant combustion process. A Launch Acoustics Measuring System allows the measurement of the acoustic field from the launch point to a distance of 15 miles and from ground level to a height of 500 feet. It can also measure structural vibration so that air to structure coupling can be determined and studied.

Conclusion

A survey has been made of measurement techniques used to determine environmental pressure and thermal parameters of an aborted launch; it was shown how a representation of the environment can be synthesized from the interpretation of these measurements. Extension of these methods to the measurement of normal launch hazards was indicated. The data acquisition and handling approaches described in this paper supply a basis for the engineering design or evaluation of materials, assemblies, and systems

subjected to the hazards of a launch and expected to survive.

Acknowledgements

Most of the analytical derivations on which the conclusions of this paper are based were performed by B. E. Bader and D. M. Webb of the Sandia Corporation Dynamics Analysis Division 1541.

Many of the PAMS design concepts are due to Frank D. Kite of the Sandia Aerospace Nuclear Safety Division 9312; his relentless drive contributed much to the realization and the success of PAMS and its improvements. The Launch Hazards Assessment Program at the US Air Force Eastern Test Range is sponsored by the ETR Range Safety Division and is implemented by Pan American World Airways/Guided Missiles Range Division under Contract AF 08(606)-7500.

References

1. Launch Hazards Assessment Program, Data Report on Test 205, PAA Engineering

2. Launch Hazards Assessment Program, Report on Atlas/Centaur Abort, Sandia Corp/PAA

3. "Blast and Fireball Comparison of Cryogenic and Hypergolic Propellants," Aerojet-General Corporation, 0822-01(01)FF, dtd June 1965

4. Abortive Missile Report (Damage Assessment) Test 205, PAA Operations Evaluation

5. Explosive Shocks in Air, G. F. Finney, Macmillan, New York, 1962

6. The Effects of Nuclear Weapons, S. Glasstone, ed., USG Printing Office, Washington, D.C. 1962

FRONTISPIECE - BEGINNING OF FIREBALL

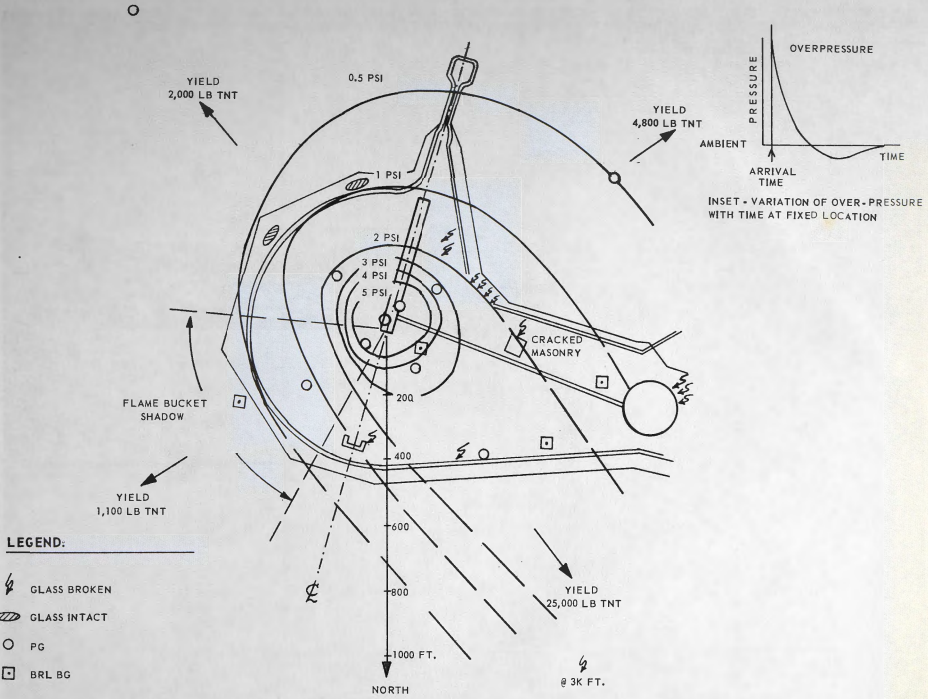

FIG. 1 PEAK OVERPRESSURE ISOBARS (3RD EXPLOSION)

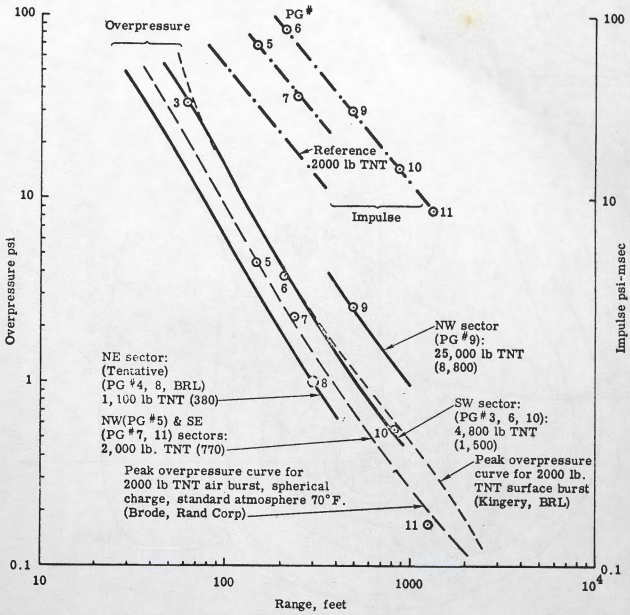

Fig. 2 OVERPRESSURE AND IMPULSE VERSUS RANGE AND EQUIVALENT YIELD VALUES (3RD EXPLOSION)

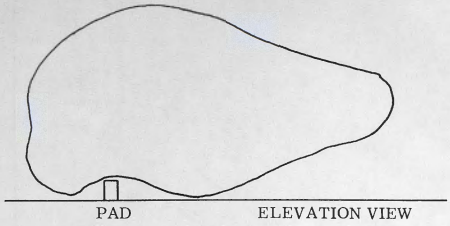

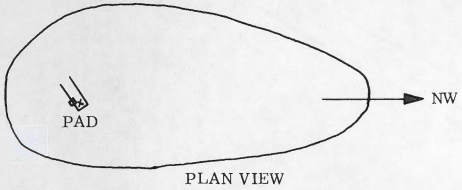

FIG. 3 SHOCKFRONT PROFILE

Fig. 4 SEARCHLIGHTS DAMAGED BY SHOCKWAVE

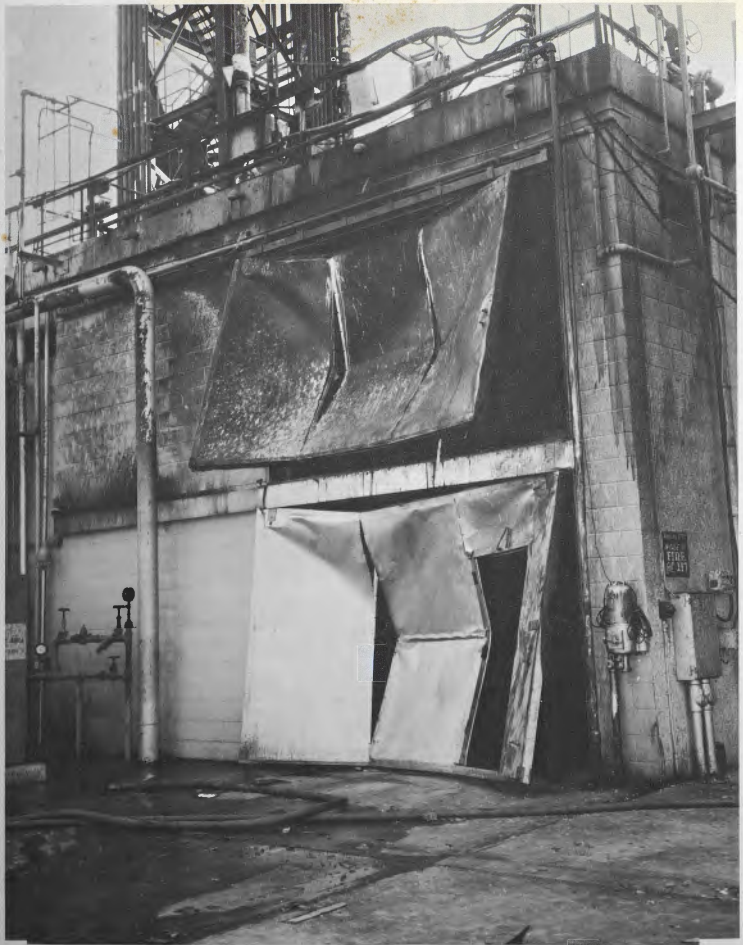

Fig. 5 COLLAPSED DOORS UNDER LAUNCH DECK DUE TO OVERPRESSURE

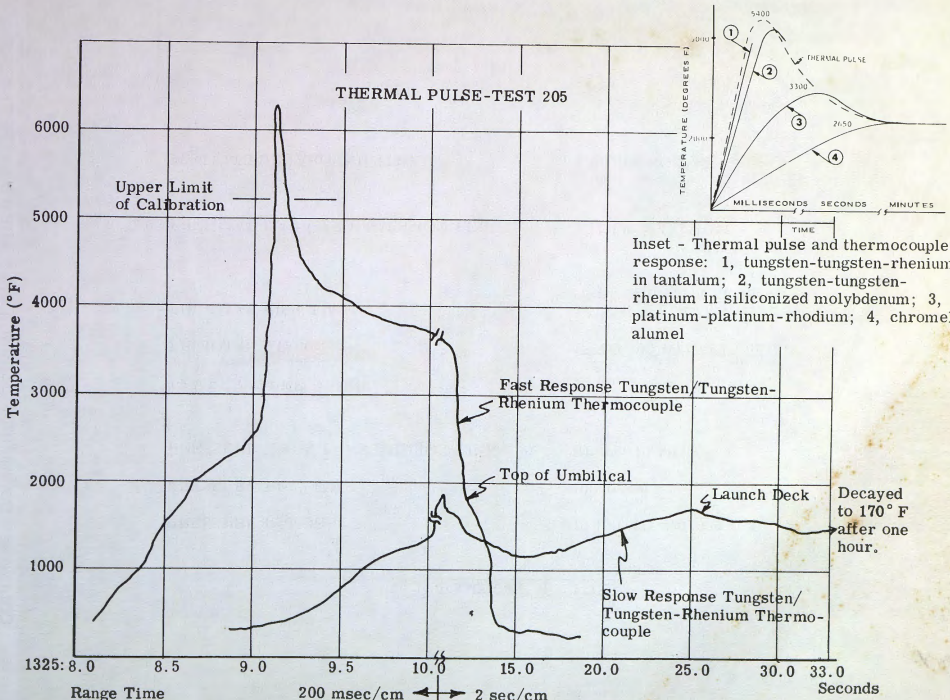

Inset - Thermal pulse and thermocouple response: 1, tungsten-tungsten-rhenium in tantalum; 2, tungsten-tungsten-rhenium in siliconized molybdenum; 3, platinum-platinum-rhodium; 4, chromel-alumel

Fig. 6 THERMAL PULSE

PAMS CAPABILITIES

PRESSURE RANGE	-10 PSI TO +20, 000 PSI
PRESSURE RISE TIME	100 USEC
PRESSURE DATA TRANSMISSION LINK	UP TO 10 MILES
TEMPERATURE RANGE	150° TO 5200 F
THERMAL FLUX	15 TO 800 BTU/FT^2 SEC
THERMAL RISE TIME	1 MSEC TO SEVERAL SECONDS DEPENDING ON SENSOR
THERMAL DATA TRANSMISSION LINK	1 MILE MAXIMUM
SYSTEM TURNAROUND TIME	4 WORKING DAYS

Fig. 7

AERIAL VIEW OF COMPLEX 36 A, PAMS SENSOR LOCATION

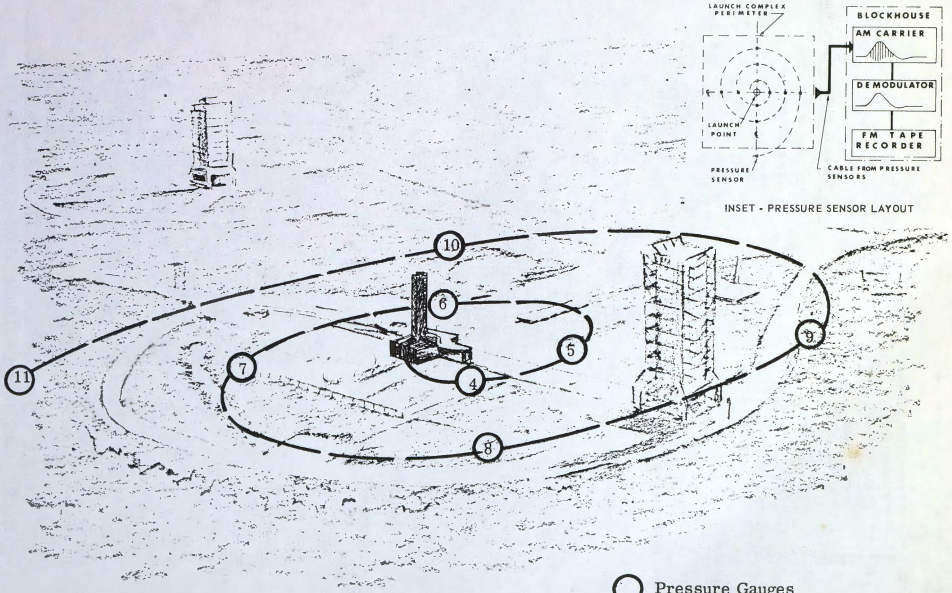

FIG. 8

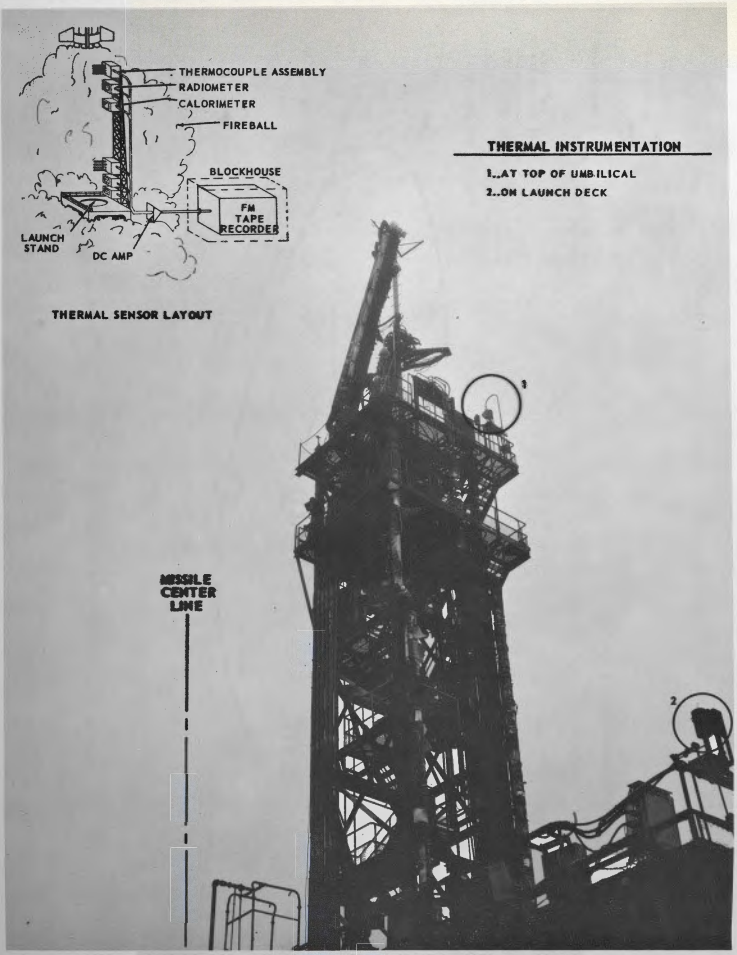

FIG. 9 PAMS THERMAL INSTRUMENTATION AT COMPLEX 36 A

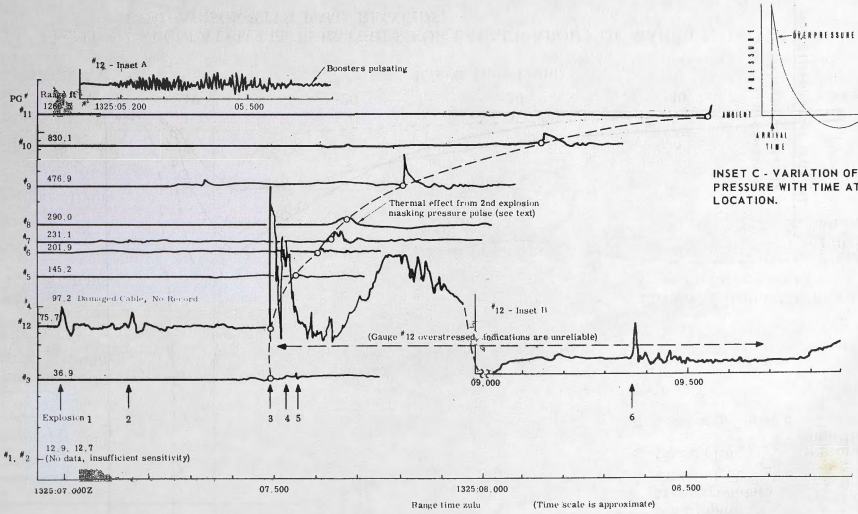

FIG. 10 PRESSURE VARIATIONS AT EACH PRESSURE GUAGE

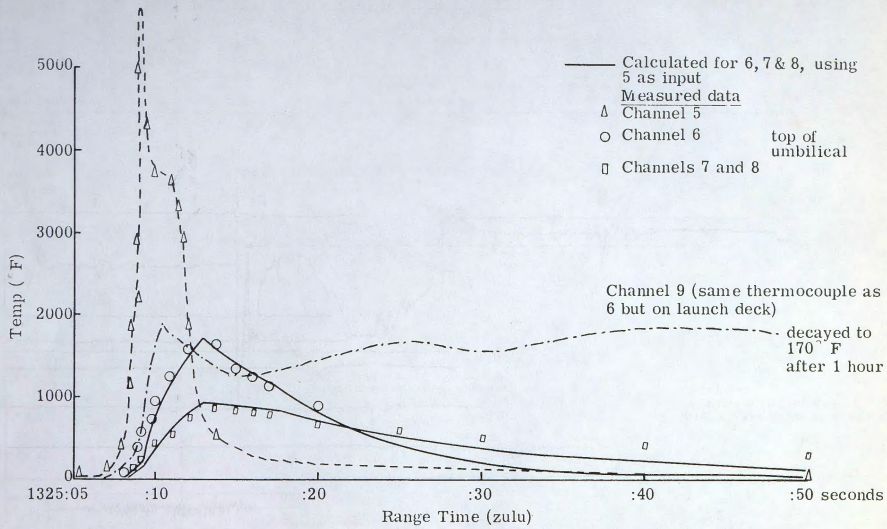

Fig. 11 CALCULATED TEMPERATURES FOR LAUNCH ABORT OF MARCH 2, 1965 AND COMPARISON WITH PAMS RECORDS.

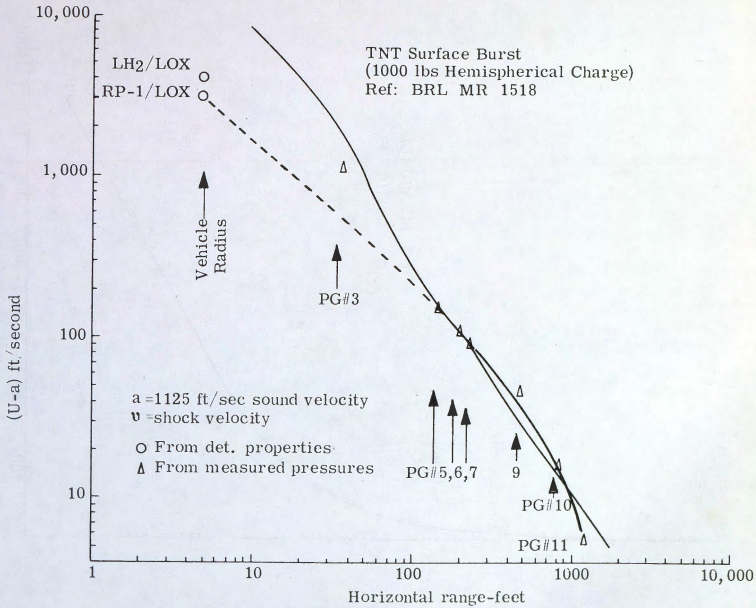

Fig. 12 RELATIVE SHOCK VELOCITY VS RANGE FOR RP-1/LOX EXPLOSION AND FOR TNT SURFACE BURST

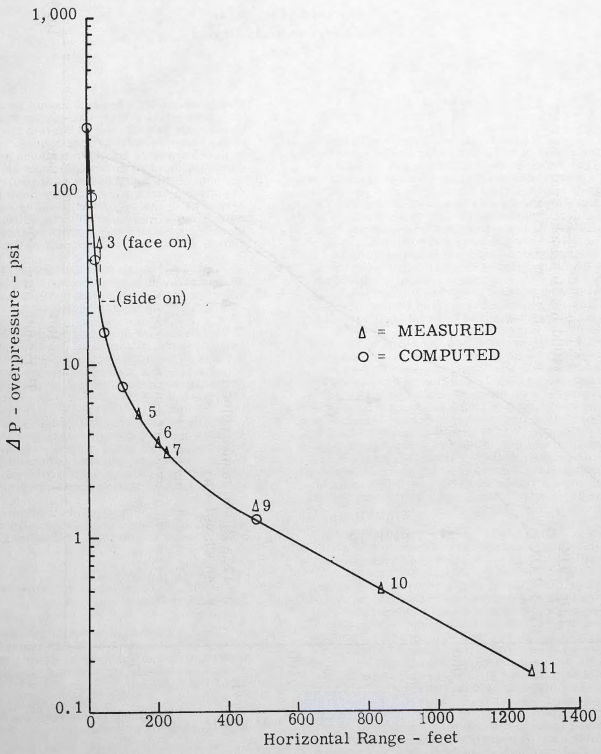

Fig. 13 TEST NO. 205 ATLAS CENTAUR ABORT OVERPRESSURE VS RANGE